Nanoparticle-Mediated Delivery of shRNA.VEGF-A Plasmids Regresses Corneal Neovascularization

Yureeda Qazi,[1,4] *Brian Stagg,*[2,4] *Nirbhai Singh,*[1] *Swita Singh,*[3] *Xiaohui Zhang,*[1] *Ling Luo,*[1] *Jacquelyn Simonis,*[1] *Uday B. Kompella,*[3] *and Balamurali K. Ambati*[1]

Purpose. To determine the efficacy of a plasmid containing a small hairpin RNA expression cassette (pSEC.shRNA) against VEGF-A–loaded poly(lactic co-glycolic acid) nanoparticles (PLGA NPs) in the sustained regression of murine corneal neovascularization.

Methods. PLGA nanoparticles were loaded with pSEC.shRNA.-VEGF-A plasmids using the double emulsion-solvent evaporation method. KNV was induced in BALB/c mice by mechanical-alkali injury. Four weeks after induction of KNV, the mice were randomly divided to receive one of four treatments intrastromally: pSEC.shRNA.VEGF-A PLGA NPs (2 μg plasmid); naked pSEC.shRNA.VEGF-A plasmid only (2 μg plasmid); control blank PLGA NPs (equivalent dry weight of NPs); and vehicle. Two and five days after intervention, corneas were harvested to determine VEGF-A gene and protein expression using reverse transcriptase polymerase chain reaction and ELISA, respectively. Four weeks after intervention, corneas were photographed, mice sacrificed, and the corneal whole mounts were immunostained for CD31 (panendothelial cell marker). Immunofluorescence microscopy was performed and the neovascular area was quantitated.

Results. VEGF-A mRNA (49.6 ± 12.4 vs. 82.9 ± 6.0%, $P < 0.01$) and protein (4.0 ± 5.2 vs. 20.0 ± 7.5 ρg VEGF-A/mg total protein, $P < 0.05$) expression were significantly reduced in pSEC.shRNA.VEGF-A PLGA NP–treated corneas as compared with control blank NP. The pSEC.shRNA.VEGF-A PLGA NP–treated corneas showed significant regression in the mean fractional areas of KNV (0.125 ± 0.042; 12.5%, $P < 0.01$) compared with both naked plasmid only (0.283 ± 0.004; 28.3%) and control (blank NPs = 0.555 ± 0.072, 55.5%) at 4 weeks post-treatment.

Conclusions. The pSEC.shRNA.VEGF-A-loaded PLGA NPs are an effective, nonviral, nontoxic, and sustainable form of gene therapy for the regression of murine KNV. (*Invest Ophthalmol Vis Sci.* 2012;53:2837–2844) DOI:10.1167/iovs.11-9139

From the [1]John A. Moran Eye Center and [2]School of Medicine, University of Utah, Salt Lake City, Utah; and the [3]Department of Pharmaceutical Sciences, School of Pharmacy, University of Colorado Denver, Aurora, Colorado.

[4]These authors contributed equally to the manuscript.

Supported by NEI Grant 5R01EY017950, NEI Grant 5R01EY017182, and a VA Merit Award to BKA.

Submitted for publication November 23, 2011; revised February 28, 2012; accepted March 21, 2012.

Disclosure: **Y. Qazi**, None; **B. Stagg**, None; **N. Singh**, None; **S. Singh**, None; **X. Zhang**, None; **L. Luo**, None; **J. Simonis**, None; **U.B. Kompella**, None; **B.K. Ambati**, None

Corresponding author: Balamurali K. Ambati, John A. Moran Eye Center, 65 Mario Capecchi Drive, Salt Lake City, UT 84132; Phone: 801-581-2352, Fax: 801-581-3357; bala.ambati@utah.edu.

Angiogenesis is a critical feature of ocular disorders such as corneal neovascularization, macular degeneration, and diabetic retinopathy.[1–3] Corneal avascularity promotes corneal transparency and thus clarity of vision.[4,5] However, insults to the ocular surface such as corneal infection, chemical injury, trauma, and rejection of corneal transplants can induce corneal neovascularization, thereby compromising vision.[3] Given that patients typically present after the onset of neovascularization, a sustainable nontoxic therapy that induces regression of pathologic corneal blood vessels is an unmet medical need.

Treatments for corneal neovascularization that have met with limited success include topical corticosteroids, topical bevacizumab, methotrexate, low-molecular-weight heparin sulfate, nonsteroidal anti-inflammatory agents, laser photocoagulation, and needle diathermy.[3,6–10] Additionally, gene therapy approaches modulating genes such as endostatin, brain-specific angiogenesis inhibitor 1, pigment epithelium-derived factor, vascular endothelial growth factor receptor-2, and vascular endothelial growth factor receptor-1 have been tested.[11–15] Another important target for anti-angiogenic gene therapy is vascular endothelial growth factor-A.[16]

VEGF-A is a key pro-angiogenic signal that plays a role in many diseases including cancer and macular degeneration.[17–19] VEGF-A promotes vascular endothelial cell migration, proliferation, inhibition of apoptosis, vasodilation, and increased vascular permeability.[20] In the cornea, angiogenesis is driven by VEGF.[21,22] Other researchers have shown that knock-down of VEGF-A expression is effective in reducing corneal neovascularization.[23,24] It has been previously demonstrated that plasmids, which express small hairpin RNA against VEGF-A, inhibit and regress corneal neovascularization.[16] However, naked plasmids are limited in their ability to treat corneal vascular diseases because of short-term delivery.

Nanoparticles (NPs) made of nonimmunogenic, biodegradable polymers such as poly(lactic co-glycolic acid) (PLGA) can deliver plasmids into the cornea in a nontoxic fashion.[15] PLGA NPs release pharmacologic agents in a sustained manner.[25–28] This slow-release, high-payload PLGA-NP system is also successful in the sustained delivery of small interfering RNAs.[29–31] Nanoparticles provide for enhanced cellular uptake and sustained delivery at the site of ocular administration.[32] The noncationic properties of PLGA NPs circumvent the issues of toxicity associated with cationic polymers. These biologically desirable physicochemical properties, in addition to the fact that PLGA is FDA approved in many pharmaceutical products, make PLGA NPs a highly translatable system once proved efficacious for its intended purpose.[33]

This study hypothesized that loading PLGA NPs with a plasmid containing an shRNA expression cassette against VEGF-A (pSEC.shRNA.VEGF-A) would constitute an enhanced and sustainable anti-angiogenic therapeutic strategy to regress corneal neovascularization after mechanical-alkali injury in a murine model of corneal injury. This study further demonstrated that pSEC.shRNA.VEGF-A PLGA NPs were able to

regress corneal neovascularization in a more sustained and robust manner than naked plasmids alone, making them a promising in vivo nonviral gene therapy tool for sustainable, nonimmunogenic, and efficacious regression of corneal neovascularization.

Methods

Animals

All animals were treated according to the ARVO Statement for the Use of Animals in Ophthalmic and Vision Research and in compliance with the University of Utah Institutional Animal Care and Use Committee (IACUC) guidelines. All experiments were performed on 6- to 8-week-old female BALB/c mice ordered from the Jackson Laboratory.

Preparation of Plasmids

Plasmids designed to induce the production of shRNA against VEGF-A have previously been described.[16] The sequence coding for shRNA inhibition of VEGF-A (AATGCAGACCAAAGAAAGACA) was inserted into pSEC Neo Vector, after which this construct was transfected into *Escherichia coli. E. coli* glycerol stocks were transformed with XL-10-Gold Ultracompetent Cells (Stratagene, La Jolla, CA) as per manufacturer's instructions using 1 ng of plasmid and the transformation mixture was plated onto Luria-Bertani agar plates with ampicillin (100 μg/mL from 100 mg/mL stock) for growth overnight at 37°C. A single colony was selected from the recombinant colonies on LB agar-ampicillin plates. The plasmids were then purified using a commercially available kit (Plasmid Mega Prep kit; Qiagen, Valencia, CA). The final concentration of plasmid used for intracorneal delivery was 1 μg/μL, with a total volume of 2 μL (2 μg of plasmid) delivered per eye.

Development of Nanoparticles

The preparation of poly-lactic co-glycolic acid nanoparticles using the double emulsion-solvent evaporation method has previously been described.[34] In summary, the anti-VEGF-A plasmids were dissolved in Tris-EDTA buffer and added to the organic phase of PLGA dissolved in dichloromethane containing Nile red and sonicated using a probe sonicator on ice. The emulsion was poured in a solution of 2% polyvinyl alcohol and sonicated again. The double emulsion was then poured into 2% PVA and the solvent was removed using evaporation, followed by centrifugation. The pellet was then re-suspended in double-distilled water and lyophilized.

Immediately prior to intracorneal administration, plasmid-loaded or blank PLGA NPs were reconstituted in vehicle (DMSO) and vortexed briefly. Based on previous successes with this plasmid,[16] the final concentration of reconstituted pSEC.shRNA.VEGF-A PLGA NPs was 1 μg/μL, with a total delivery volume of 2 μL per eye (2 μg plasmid).

Determination of Plasmid Loading

Determination of plasmid loading of PLGA NPs had also been described.[34] In brief, 1mg of PLGA NPs were placed in glass Kimble tubes after lyophilization. These were dissolved in dichloromethane, mixed with water, vortexed at high speed, and allowed to separate into an organic and aqueous phase. The aqueous phase was collected and analyzed using UV spectrophotometry to determine the concentration of plasmid. Nanoparticles had a plasmid loading of 18.45 μg plasmid/mg of nanoparticles.

Mechanical-Alkali Trauma Model

In order to induce corneal neovascularization, the established murine mechanical-alkali trauma model was used.[15] In this model, after induction of general anesthesia by inhalation of isoflurane (0.3 mL isoflurane on gauze), a drop of topical proparacaine, and tropicamide were applied to the mouse cornea for topical anesthesia and mydriasis. Thereafter, 2 μL of 0.2 M sodium hydroxide was applied to corneas of anesthetized BALB/c mice for 10 seconds. A corneal knife (Tooke; Katena Products, Denville, NJ) was used to gently scrape the corneal and limbal epithelium of each cornea under a light biomicroscope (SZX7 Zoom Stereomicroscope; Olympus, Center Valley, PA). The corneas were rinsed with phosphate buffered saline to wash away any remaining alkali. Topical erythromycin ophthalmic ointment was then applied to the corneas after epithelial removal to prevent infection and the mice were returned to a heating pad for recovery. Following mechanical-alkali injury, the growth of blood vessels was allowed to proceed and mature over the course of four weeks.

Corneal Intrastromal Injections

Delivery of both naked plasmids and NPs to the cornea via intrastromal injection has been described.[15,35] This mode of delivery was specifically chosen for its ability to allow controlled delivery of a specific amount of deliverables directly to the site of pathology. Under a light biomicroscope, a 0.5-inch, 30-gauge needle (BD Biosciences, Franklin Lakes, NJ) was first used to create a nick in the epithelium and anterior stroma near the midperiphery of the mouse corneas while the animal was under general (ketamine 33.3 mg/mL and xylazine 2.14 mg/mL in PBS; 0.003 mL ketamine-xylazine-PBS cocktail/g body weight of mouse, intraperitoneally) and topical anesthesia (proparacaine) with mydriasis (tropicamide). Care was taken not to puncture the cornea. Following this, a 31-gauge needle with a 30° bevel on a 10-μL gas-tight syringe (Hamilton, Reno, NV) was gently inserted through the nick towards the central corneal stroma. Once inserted and positioned, 2 μL of solution was forcibly injected into the corneal stroma. Successful intrastromal injections were visualized using Nile red dye loading in nanoparticles.

Four weeks after corneal mechanical-alkali injury, the BALB/c mice were randomly divided into four treatment groups: PLGA NPs carrying pSEC.shRNA.VEGF-A (2μg plasmid/eye); naked pSEC.shRNA.VEGF-A plasmid (2 μg plasmid/eye); blank PLGA NPs (2 μL/eye); and vehicle (2 μL/eye). One cornea of each mouse received one intrastromal injection of the respective treatment group at 4 weeks post-mechanical alkali injury. Brightfield photographs of mouse corneas were taken 4 weeks pre- and post-treatment using a light microscope attached to a digital camera (SZX7 Zoom Stereomicroscope, Olympus, Center Valley, PA).

Reverse Transcriptase Polymerase Chain Reaction

Mice from each treatment group were euthanized by CO_2 inhalation 2 days after intrastromal injection for analysis of VEGF-A mRNA expression using reverse transcriptase polymerase chain reaction ($n = 4$–5 corneas/group). Corneas were harvested, rinsed in cold PBS, and immediately placed in an RNA-stabilizing agent (RNAlater; Qiagen, Valencia, CA). The tissue was then processed using gentle sonication and RNA extracted as per manufacturer's instructions using a commercially available kit (RNeasy Mini Kit; Qiagen, Valencia, CA). One-step RT-PCR was performed using 100 ng of RNA in a 50-μL reaction mixture as per manufacturer's instructions (QIAGEN OneStep RT-PCR Kit; Valencia, CA) with a 0.6-μm final concentration of primers. Primers were designed to amplify mouse VEGF-164 (forward: 5′-TCACCAAAGCCAGCACATAGGAGA- 3′; reverse: 5′-TTCGTTTAACTCAAGCTGCCTCGC-3′; product size 211 base pairs; Integrated DNA Technologies Inc., Coralville, IA), and the housekeeping gene, glyceraldehyde 3-phosphate dehydrogenase (forward: 5′-AACTTTGGCATTGTGGAAGGG-3′; reverse: 5′-ACCAGTGGATGCAGGGATGAT-3′; product size 138 base pairs; Integrated DNA Technologies Inc., Coralville, IA). Reverse transcription was performed at 50°C for 30 minutes followed by heat start activation of DNA polymerase at 95°C for 15 minutes. All RT-PCR reactions were run in a thermal cycler (Eppendorf, Hauppauge, NY) for 35 cycles with denaturing at 94°C for 30 seconds, annealing at 55°C for 30 seconds and extension at 72°C for 1 minute. A final extension step at 72°C for 10 minutes was run after the cycles were completed. DNA gel electropho-

resis was performed to resolve the amplified RT-PCR products using a 2% agarose gel, loading 5 μL of sample per lane. VEGF-A gene expression was quantitated by densitometric analysis (ImageJ) of the ethidium bromide-stained gel images acquired using a transilluminator attached to a digital camera (FOTO/Analyst Investigator/Eclipse System; FOTODYNE, Hartland, WI; C8484 digital camera; Hamamatsu Photonics, Bridgewater, NJ). VEGF-A gene expression was standardized with GAPDH gene expression. Results were expressed as mean percentage of VEGF-A/GAPDH gene expression ± SD. Student's *t*-test was used to statistically analyze the results.

ELISA

Mice from each treatment group were euthanized by CO_2 inhalation 5 days after intrastromal injection for determination of VEGF-A protein expression using ELISA ($n = 68$ corneas/group). Corneas were harvested and two corneas were pooled and placed in 180 μL of cell lysis and protein solubilization buffer (RIPA Buffer; Sigma-Aldrich, product number R0278, Sigma-Aldrich, St. Louis, MO) with a protease inhibitor (SigmaFAST, protease inhibitor cocktail tablet, Sigma-Aldrich, St. Louis, MO), after which the corneas were homogenized using sonication. Pooling of corneas was done to achieve measurable levels of VEGF-A. The homogenate was centrifuged and the supernatant collected for protein estimation. A bicinchoninic acid protein assay (Pierce BCA Protein Assay Kit; catalog number 23225, Thermo Fisher Scientific, Rockford, IL) was used as per manufacturer's instructions to determine total protein content of the samples.

Total levels of VEGF-A in the samples were determined using a commercially available ELISA kit (Quantikine; Mouse VEGF Immunoassay, catalog number MMV00, R&D Systems, Minneapolis, MN) as per manufacturer's instructions. Briefly, 50 μL of each of the standards (VEGF-A positive control); controls (vehicle and blank NP–treated corneal homogenates); and samples (plasmid and plasmid-NP–treated corneal homogenates) were carefully loaded onto a 96-well plate containing an assay diluent. The plate was incubated for 2 hours at room temperature on a shaker and then washed gently five times. A 100 μL of mouse VEGF conjugate solution was then added to the wells, followed by incubation for 2 hours at room temperature on a shaker and five washes. Following the last wash, 100 μL of substrate solution was added and incubated for 30 minutes in the dark at room temperature. After the 30-minute incubation, 100 μL of stop solution was added to all wells and the optical density read at 450 nm using a microplate reader (BioTek, Winooski, VT), with a second reading taken at the correction wavelength of 540 nm. All experiments were performed in duplicate. VEGF-A concentration of each sample was calculated from the standard curve and standardized using total protein concentrations determined by the BCA assay described earlier. Student's t-test was used for statistical analysis.

Immunostaining of Corneal Whole Mounts

Mice from each group were sacrificed 4 weeks after injection for preparation of corneal whole mounts for vascular staining ($n = 2$–4 corneas/group). The method used for whole mount preparation and staining has been described.[15] After euthanasia using CO_2 inhalation, corneas were harvested from the mice and washed with PBS for 30 minutes on a shaker at 4°C, followed by fixation with 100% acetone for 20 minutes on a shaker at room temperature. After fixation, the corneas were rinsed four times for 10-minute periods with PBS-0.05% polysorbate 20 (Tween20, product number P1379; Sigma-Aldrich, St. Louis, Missouri) at room temperature on a shaker. To prevent nonspecific binding, the corneas were blocked with 3% bovine serum albumin-PBS (0.1 M PBS; BSA, Sigma-Aldrich, St. Louis, MO) overnight at 4°C on a shaker for 3 nights. Corneas were then incubated with FITC-conjugated monoclonal rat anti-mouse CD31 antibody (material number 558736; clone 390; BD Pharmingen, San Diego, CA) at a concentration of 1:500 constituted in 3% BSA-PBS at 4°C overnight in the dark on a shaker. After staining, the corneas were washed with PBS-0.05% polysorbate 20 (Sigma-Aldrich) at room temperature for four 10-minute periods on a shaker and then mounted with an antifading agent (Gel Mount; Biomedia, Inc, San Francisco, CA). Images were acquired using a fluorescence microscope (Zeiss, Oberkochen, Germany) attached to a digital camera (AxioCam MRc5; Zeiss, Oberkochen, Germany).

Quantitation of Neovascularization

Corneal neovascularization of whole mounted corneas was quantitated using previously described methods.[15] Images acquired were converted to tagged information file format files at 624 × 480 pixel resolution. These TIFF files were then analyzed using Scion Image. The researcher performing the analysis was blinded to the treatment arms of each image. The area of neovascularization was determined by converting the colored images to black and white, applying binary mode, and setting a contrast threshold level above which only vessels were visualized. The total corneal area was then outlined, using the interior edge of the limbus as the external border. The neovascular (black pixels) and avascular (white pixels) areas were determined, and the fractional neovascular area calculated (corneal neovascular area/total corneal area). Results were reported as mean fractional area ± SD. Statistical analysis was performed using Student's t-test.

Results

shRNA.VEGF-A PLGA Nanoparticles Reduce VEGF-A Gene Expression

Intrastromal injections of both treatments delivering 2 μg of plasmid either by PLGA NPs loaded with pSEC.shRNA.VEGF-A plasmid, or, naked pSEC.shRNA.VEGF-A plasmid alone, significantly reduced the expression of VEGF-A mRNA in the cornea compared with controls (Figs. 1A, 1B). The control groups, vehicle and blank NP, had VEGF-A gene expression levels of 77.7 ± 18.9% ($n = 4$) and 82.9 ± 6.1% ($n = 5$), respectively (Fig. 1B), while the treatment groups, pSEC.shRNA.VEGF-A NP and naked plasmid, had considerably reduced VEGF-A gene expression of 49.6 ± 12.4%, ($P < 0.05$, $n = 4$) and 44 ± 13.4%, ($P < 0.05$, $n = 5$), respectively. There was no statistically significant difference in the VEGF-A gene expression levels of controls ($P > 0.05$). At day 2 post-intrastromal injection, both the naked plasmid- and the slow-release NP-encapsulated plasmid-treated groups had comparable VEGF-A mRNA expression (44 ± 13.4%, $n = 5$; 49.6 ± 12.4%, $n = 4$, $P > 0.05$). This suggested that PLGA-NPs released some encapsulated plasmid soon after in vivo injection, matching the extent of early gene silencing observed by a naked plasmid.

shRNA.VEGF-A PLGA Nanoparticles Reduce VEGF-A Protein Expression

Intrastromal injection of shRNA.VEGF-A-loaded PLGA NPs delivering 2 μg of plasmid significantly reduced corneal VEGF-A protein expression (Fig. 2) as compared with naked plasmid (4.0 ± 5.2 vs. 16.1 ± 7.2 ρg VEGF-A/mg total protein, $n = 4$, $P < 0.05$) and blank NP control (4.0 ± 5.2 vs. 20.0 ± 7.5 ρg VEGF-A/mg total protein, $n = 4$, $P < 0.05$). While the naked plasmid-treated corneas demonstrated a trend towards reduction of total VEGF-A protein expression compared to blank NP control (16.1 ± 7.2 vs. 20.0 ± 7.5 ρg VEGF-A/mg total protein, $n = 3$, $P > 0.05$), it did not achieve statistical significance (Fig. 2). With reference to the control blank NP–treated group (20.0 ± 7.5 ρg VEGF-A/mg total protein, $n = 4$), corneas treated with NP-encapsulated shRNA.VEGF-A plasmid (4.0 ± 5.2 ρg VEGF-A/mg total protein, $n = 4$, $P < 0.05$) and naked plasmid alone (16.1 ± 7.2 ρg VEGF-A/mg total protein, $n = 3$, $P > 0.05$), demonstrated respective reductions in total VEGF-A protein

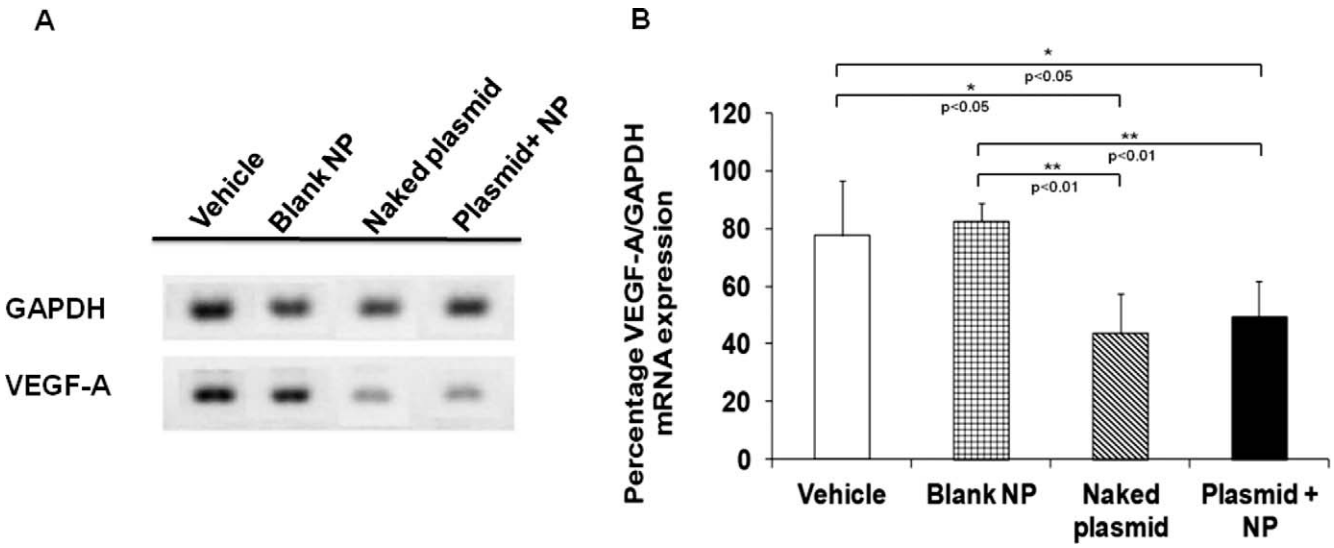

Figure 1. shRNA.VEGF-A NPs inhibit expression of VEGF-A mRNA. RT-PCR was performed on vascularized corneas harvested 2 days post-intrastromal injection of treatment or control ($n = 4$–5 corneas/group), to study gene expression profiles of VEGF-A ($VEGF_{164}$). GAPDH was used as the housekeeping gene. (**A**) Representative image of DNA gel electrophoresis for GAPDH and VEGF-A from RT-PCR products across the experiment groups. (**B**) Quantitation of VEGF-A gene expression as a ratio of GAPDH gene expression, determined by densitometric analysis of DNA gel electrophoresis using ImageJ. All values are reported as mean ± SD. $P < 0.05$ is considered statistically significant.

expression by 79.9% and 19.7%, even though the latter was not statistically significant.

shRNA.VEGF-A PLGA Nanoparticles Regress Corneal Neovascularization

Fluorescence microscopy of immunostained corneal whole mounts harvested 4 weeks after intrastromal injection revealed significant regression of KNV in corneas treated with pSEC.shRNA.VEGF-A PLGA-NPs and naked pSEC.shRNA.-VEGF-A plasmid as compared with controls, blank NPs, and vehicle (Figs. 3A–E). Systematic analysis of KNV area showed that corneas treated with pSEC.shRNA.VEGF-A NPs and naked plasmid had mean fractional areas of 0.125 ± 0.042 ($n = 4$, $P < 0.01$) and 0.283 ± 0.0004 ($n = 2$, $P < 0.01$), respectively (Fig. 3E). However, the control groups, blank NP, and vehicle-treated corneas, had mean fractional areas of 0.555 ± 0.072 ($n = 4$) and 0.5304 ± 0.044 ($n = 4$), respectively (Fig. 3E). There was no statistically significant difference in the mean fractional area of KNV between the control groups. While both the naked plasmid and NP-encapsulated shRNA.VEGF-A plasmid induced statistically significant regression of KNV compared with controls, the greatest regression in KNV was observed with the sustained release mechanism of the shRNA.VEGF-A–conjugated NPs (0.125 ± 0.042, $n = 4$, $P < 0.01$). Brightfield microscopy of mouse corneas 4 weeks pre- and post-intrastromal injection also revealed a remarkable phenotypic difference in KNV between the vehicle (Figs. 4A, B), and sustained delivery pSEC.shRNA.VEGF-A–NP treatment groups (Figs. 4C, D). The brightfield micrograph (Fig. 4D) shows regression of blood vessels especially along the central visual axis, which is pertinent for clear vision.

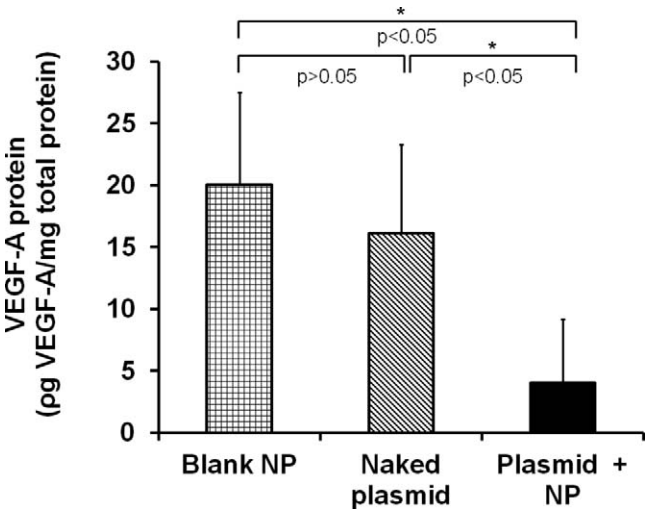

Figure 2. shRNA.VEGF-A NPs inhibit expression of VEGF-A protein. ELISA for total VEGF-A was performed on homogenates of vascularized corneas at 5 days after intrastromal injection with respective treatment or control (n = 3–4/group; 6–8 corneas/group). Results were normalized by total protein content measured by the bicinchoninic assay (BCA Bio-Rad, Hercules, CA) There was no significant difference between corneas treated with naked plasmid and control. However, NP-encapsulated plasmid-treated corneas demonstrated significant reduction in free VEGF-A protein levels in comparison with naked plasmid and control. With reference to control, naked plasmids and NP-encapsulated plasmids decreased VEGF-A protein expression by 19.7% and 79.9%, respectively. All values are reported as mean ± SD. $P < 0.05$ is considered statistically significant.

Discussion

RNA interference is an effective gene silencing technique to retard ocular neovascularization.[16,24,36,37] shRNAs present a far more attractive alternative to siRNAs given their ability to avoid and minimize off-target effects such as nonspecific, generalized immune activation through toll-like receptor 3 activation, a common off-target effect of siRNAs.[38] TLR 3 is activated by double-stranded RNAs, such as siRNAs; but its activation can be avoided by the use of shRNAs, which form a construct within a DNA plasmid. Bypassing TLR 3 activation lends shRNAs the benefit of preventing immune-mediated inflammation through interferons and interferon-stimulated gene activation. This mechanism becomes increasingly important in devising anti-angiogenic strategies free of nonspecific off-target effects.

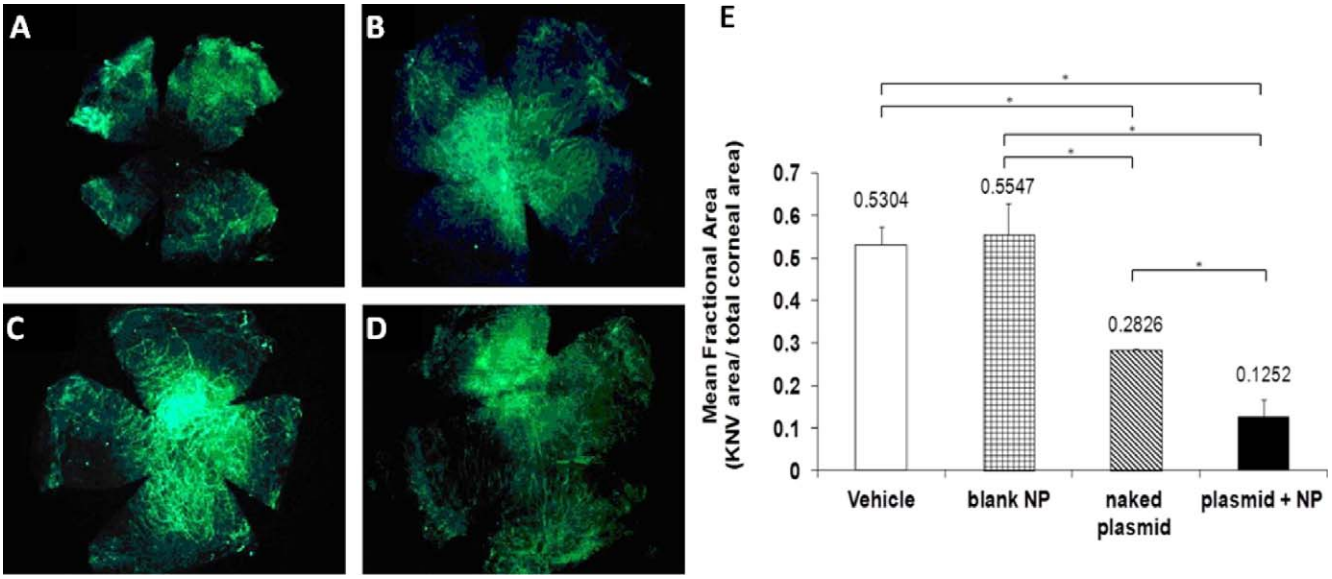

Figure 3. shRNA.VEGF-A NPs regress KNV**.** Immunostaining for CD31 (panendothelial marker) was performed on vascularized corneas harvested at four weeks post-intrastromal injection with either treatment or control. Images of immunostained corneal whole mounts were acquired using a fluorescence microscope. **(A–D)** Representative fluorescence micrographs of CD31-immunostained corneal whole mounts 4 weeks post-intrastromal injection with pSEC.shRNA.VEGF-A PLGA NP (A, $n = 4$); naked plasmid (B, $n = 2$); blank PLGA NP (C, $n = 4$); and vehicle (D, $n = 4$). **(E)** Quantitation of the mean fractional area of corneal neovascularization from immunostained corneal whole mounts harvested after 4 weeks post-intrastromal delivery of either treatment or control. NP-encapsulated anti-VEGF-A plasmids demonstrated the greatest efficacy at regression of murine corneal neovascularization (0.125 ± 0.042, $P < 0.01$) compared with naked plasmid (0.283 ± 0.004, $P < 0.01$) and controls (0.555 ± 0.072; 0.530 ± 0.044; $P > 0.05$). All values are reported as mean $\pm$ SD. $P < 0.05$ is considered statistically significant.

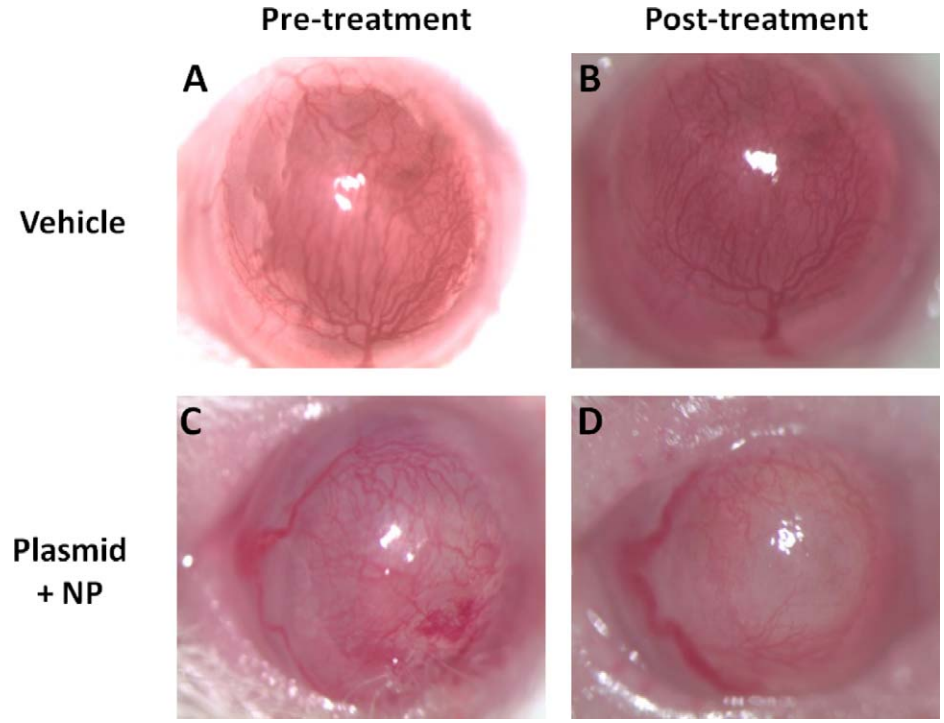

Figure 4. KNV regression on brightfield microscopy. Representative brightfield micrographs of mouse corneas. **(A)** Corneas treated with vehicle, pre-treatment. **(B)** Cornea treated with vehicle 4 weeks post-treatment. **(C)** Cornea treated with pSEC.shRNA.VEGF-A PLGA NPs, pre-treatment. **(D)** Cornea treated with pSEC.shRNA.VEGF-A PLGA NPs, 4 weeks post-treatment. Unlike with the vehicle-treated corneas **(B)**, regression of corneal neovascularization, especially along the central visual axis, was observed in corneas injected with anti-VEGF-A plasmid-loaded PLGA NPs (pSEC.shRNA.VEGF-A PLGA NPs) delivering 2 μg plasmid **(D)**.

Recently, it was shown that through siRNA-mediated TLR 3 activation, IFN-γ and IL-12 production lead to nonspecific anti-angiogenic effects.[39] Another mechanism by which shRNAs avoid immune activation is by virtue of their endogenous splicing unlike that of siRNAs.[40,41] Hence, shRNAs present a relatively nonimmunogenic as well as a more specific, targeted anti-angiogenic strategy, making it a translational tool for anti-angiogenic gene therapy. However, the therapeutic application of shRNA technology is restricted by the lack of a nonviral, nontoxic, sustainable, and efficacious vector for delivery. To that end, the combinatorial efficacy of nonviral and biodegradable PLGA nanoparticles loaded with shRNA against VEGF-A was investigated. This approach is currently being tested in the laboratory in other models of neovascularization as well, such as murine models of age-related macular degeneration.

PLGA NPs have been successfully used to deliver shRNAs in vitro with sustained effects and absence of toxicity.[42] Previous studies have demonstrated the entry of NPs into corneal cells following intrastromal injections.[15] By employing intrastromal injections to deliver NPs or controls, this study found that both naked and PLGA NP–encapsulated pSEC.shRNA.VEGF-A plasmids caused a comparable decrease in the level of VEGF-A mRNA in neovascularized corneas (Fig. 1). However, compared with naked plasmids, the pSEC.shRNA.VEGF-A PLGA NPs induced a greater reduction in total VEGF-A protein expression and regression of KNV (Fig. 2). This significant decrease in total corneal VEGF-A protein expression by pSEC.shRNA.VEGF-A PLGA NPs likely led to the phenotypic regression of KNV, as supported by the pivotal role of VEGF-A in KNV.[21,22] Unlike corneas treated with naked plasmid alone, the phenotypic regression of KNV seen in the pSEC.shRNA.VEGF-A NP-treated group was sustained to a greater degree at 4 weeks post-intrastromal injection (Figs. 3 and 4), making pSEC.shRNA.-VEGF-A PLGA NPs an effective and sustainable form of gene therapy for the regression of murine KNV.

The primary purpose of this study's experiments was to investigate the efficacy and sustainability of combining a non-immunogenic anti-angiogenic gene therapy strategy (shRNA.-VEGF-A) with an FDA-approved, nonviral, biodegradable vehicle (PLGA NPs) to carry the anti-angiogenic plasmid directly to the site of pathology via intrastromal injection. Since PLGA systems undergo some initial dissolution in an aqueous tissue microenvironment, this study investigated the differences in gene expression between the naked plasmid and NP-encapsulated plasmids, by assaying the respective groups for VEGF-A mRNA expression at an early time point of 2 days following injection, a time when changes in gene expression would be evident.

An interesting aspect of this study's results was the observation of a comparable degree of VEGF-A mRNA silencing by both the naked and PLGA NP-encapsulated plasmid pSEC.shRNA.VEGF-A (Fig. 1) 2 days after intrastromal injection. This finding is consistent with the recently described physicochemical properties of PLGA NPs delivering siRNAs.[29] PLGA NPs are a high-payload system; there is an initial release of plasmids located near the surface, likening their gene silencing effect to that of a naked plasmid, while maintaining its sustained release properties over time.[29] Another probable explanation could be the partial dissolution of plasmid-loaded PLGA NPs in vehicle immediately prior to intrastromal injection. This may have facilitated immediate release of some plasmids for prompt gene silencing.

Five days after intrastromal injection, pSEC.shRNA.VEGF-A PLGA NPs had established a clear advantage over naked pSEC.shRNA.VEGF-A plasmid by inducing a significantly greater reduction in total corneal VEGF-A protein expression (Fig. 2). This can be explained by the short life of naked siRNAs in vivo (5–7 days) secondary to digestion by nucleases and by the greater retention of NPs at the site of ocular administration.[32,43] PLGA NP-encapsulation of the plasmids protects them from nuclease digestion.[29] The pSEC.shRNA.VEGF-A PLGA NPs reduced total corneal VEGF-A protein expression by 79.9%.

It is believed that the pSEC.shRNA.VEGF-A PLGA NP-induced regression of KNV seen both on CD31 immunostaining of corneal whole mounts (Figs. 3A, E) and brightfield microscopy of mouse corneas (Fig. 4D) can be explained by well-established reports of endothelial cell apoptosis following knockdown of VEGF-A. VEGF-A is a key mediator of endothelial cell migration and survival. Knockdown of VEGF-A induces apoptosis in various models, and hence a promising strategy in anti-angiogenesis.[44] This study's demonstration of the sustained gene silencing effects using PLGA nanoparticles were consistent with the inherent properties of the PLGA nanoparticle system.[42,45] The PLGA nanoparticle delivery system was used in an earlier study where it was observed that intratumorally injected intraceptor plasmid-loaded PLGA nanoparticles were effective over the 7-week course of the study, supporting the sustainability of PLGA nanoparticle-mediated anti-angiogenic effects observed in this current study.[46] Furthermore, the nanoparticles used in this study were of a size of $\geq$200 nm. Nanoparticles of this size have previously been shown to exhibit remarkable retention properties of up to 2 months in the periocular space.[32] Therefore, it is anticipated that intrastromal PLGA nanoparticles are cleared slowly based on polymer degradation time, making them a practical and exciting mode of delivery for translational anti-angiogenic gene therapy.

The naked pSEC.shRNA.VEGF-A plasmid also resulted in some regression of KNV (Figs. 3B, E), although to a lesser degree. This sustained anti-angiogenic effect of the naked shRNA.VEGF-A plasmid can be explained by a possible reduction in the vessel load early after the treatment injection, which resulted in regression of KNV, albeit to a much smaller magnitude than the NP-encapsulated plasmids.

Since this study was based on a model of corneal neovascularization where the blood vessels were allowed to mature over a course of 4 weeks, the data revealing a robust and sustained regression of KNV for the tested period of 4 weeks following a single intrastromal injection of a small volume of pSEC.shRNA.VEGF-A PLGA NPs (2 μg plasmid in 2 μL vehicle) has direct relevance to patients seen in ophthalmic practice both with respect to maturity of blood vessels at the time of treatment and sustained effects of single-dose therapy. Consequently, this further underscores the promising translational potential of the tested anti-angiogenic gene therapy tool using PLGA NPs, which are approved for clinical use by the FDA.

Having demonstrated the efficacy and sustainability of this nonviral and nontoxic anti-angiogenic therapeutic strategy in vivo, it is believed that intrastromal delivery of pSEC.shRNA.-VEGF-A PLGA NPs not only has broad applications in other species (rats, rabbits) and animal models of neovascularization (AMD, diabetic retinopathy), but also possesses translational potential providing an attractive option to consider in the treatment of human corneal neovascularization. Avenues for future research stemming from the work presented in this manuscript may include determining the effects of multiple dosing and injections at multiple sites on the regression of KNV. Important future considerations for clinical trials include the determination and development of a dose-response curve, identification of optimal dosing in primates and/or humans, and investigating the possibility of any reactive vascular congestion in response to anti-angiogenic therapy. Further strengths of this proposed nonviral, sustainable anti-angiogenic gene therapy tool may lie in its broader applications to other vasculoproliferative disorders such as AMD, diabetic retinop-

athy, and systemic conditions that rely on pathological neovascularization such as cancer metastasis.

A treatment providing highly efficacious, sustainable, nontoxic regression of KNV would be valuable given the pathologic severity and sight-threatening implications of corneal neovascularization. Study results show that PLGA nanoparticles loaded with anti-VEGF-A plasmids have the capability of meeting this need. Strengths to this approach are that it is a nonviral, nonimmunogenic method of gene delivery that results in sustained release and effect.

References

1. Ciulla TA, Rosenfeld PJ. Antivascular endothelial growth factor therapy for neovascular age-related macular degeneration. *Curr Opin Ophthalmol*. 2009;20:158–165.
2. Rothenbuehler SP, Waeber D, Brinkmann CK, Wolf S, Wolf-Schnurrbusch UE. Effects of ranibizumab in patients with subfoveal choroidal neovascularization attributable to age-related macular degeneration. *Am J Ophthalmol*. 2009;147: 831–837.
3. DeStafeno JJ, Kim T. Topical bevacizumab therapy for corneal neovascularization. *Arch Ophthalmol*. 2007;125:834–836.
4. Cursiefen C. Immune privilege and angiogenic privilege of the cornea. *Chem Immunol Allergy*. 2007;92:50–57.
5. Azar DT. Corneal angiogenic privilege: angiogenic and antiangiogenic factors in corneal avascularity, vasculogenesis, and wound healing (an American Ophthalmological Society thesis). *Trans Am Ophthalmol Soc*. 2006;104:264–302.
6. Chang JH, Gabison EE, Kato T, Azar DT. Corneal neovascularization. *Curr Opin Ophthalmol*. 2001;12:242–249.
7. Gerten G. Bevacizumab (avastin) and argon laser to treat neovascularization in corneal transplant surgery. *Cornea*. 2008;27:1195–1199.
8. Joussen AM, Kruse FE, Volcker HE, Kirchhof B. Topical application of methotrexate for inhibition of corneal angiogenesis. *Graefes Arch Clin Exp Ophthalmol*. 1999;237:920–927.
9. Lepri A, Benelli U, Bernardini N, et al. Effect of low molecular weight heparan sulphate on angiogenesis in the rat cornea after chemical cauterization. *J Ocul Pharmacol*. 1994;10:273–280.
10. Mazhdrakova I, Demerdjieva Z. [Neovascularisation of the cornea]. *Klin Monatsbl Augenheilkd*. 2005;222:623–629.
11. Lai LJ, Xiao X, Wu JH. Inhibition of corneal neovascularization with endostatin delivered by adeno-associated viral (AAV) vector in a mouse corneal injury model. *J Biomed Sci*. 2007; 14:313–322.
12. Yoon KC, Ahn KY, Lee JH, et al. Lipid-mediated delivery of brain-specific angiogenesis inhibitor 1 gene reduces corneal neovascularization in an in vivo rabbit model. *Gene Ther*. 2005;12:617–624.
13. Kuo CN, Yang LC, Yang CT, et al. Inhibition of corneal neovascularization with plasmid pigment epithelium-derived factor (p-PEDF) delivered by synthetic amphiphile INTeraction-18 (SAINT-18) vector in an experimental model of rat corneal angiogenesis. *Exp Eye Res*. 2009;89:678–685.
14. Albuquerque RJ, Hayashi T, Cho WG, et al. Alternatively spliced vascular endothelial growth factor receptor-2 is an essential endogenous inhibitor of lymphatic vessel growth. *Nat Med*. 2009;15:1023–1030.
15. Jani PD, Singh N, Jenkins C, et al. Nanoparticles sustain expression of Flt intraceptors in the cornea and inhibit injury-induced corneal angiogenesis. *Invest Ophthalmol Vis Sci*. 2007;48:2030–2036.
16. Singh N, Higgins E, Amin S, et al. Unique homologous siRNA blocks hypoxia-induced VEGF upregulation in human corneal cells and inhibits and regresses murine corneal neovascularization. *Cornea*. 2007;26:65–72.
17. Backer MV, Hamby CV, Backer JM. Inhibition of vascular endothelial growth factor receptor signaling in angiogenic tumor vasculature. *Adv Genet*. 2009;67:1–27.
18. Presta LG, Chen H, O'Connor SJ, et al. Humanization of an anti-vascular endothelial growth factor monoclonal antibody for the therapy of solid tumors and other disorders. *Cancer Res*. 1997;57:4593–4599.
19. Ferrara N, Kerbel RS. Angiogenesis as a therapeutic target. *Nature*. 2005;438:967–974.
20. Ferrara N. VEGF and the quest for tumour angiogenesis factors. *Nat Rev Cancer*. 2002;2:795–803.
21. Ambati BK, Nozaki M, Singh N, et al. Corneal avascularity is due to soluble VEGF receptor-1. *Nature*. 2006;443:993–997.
22. Amano S, Rohan R, Kuroki M, Tolentino M, Adamis AP. Requirement for vascular endothelial growth factor in wound- and inflammation-related corneal neovascularization. *Invest Ophthalmol Vis Sci*. 1998;39:18–22.
23. Kim B, Tang Q, Biswas PS, et al. Inhibition of ocular angiogenesis by siRNA targeting vascular endothelial growth factor pathway genes: therapeutic strategy for herpetic stromal keratitis. *Am J Pathol*. 2004;165:2177–2185.
24. Zuo L, Fan Y, Wang F, Gu Q, Xu X. A siRNA targeting vascular endothelial growth factor-A inhibiting experimental corneal neovascularization. *Curr Eye Res*. 2010;35:375–384.
25. Golub JS, Kim YT, Duvall CL, et al. Sustained VEGF delivery via PLGA nanoparticles promotes vascular growth. *Am J Physiol Heart Circ Physiol*. 2010;298:H1959–1965.
26. Rao DA, Forrest ML, Alani AW, Kwon GS, Robinson JR. Biodegradable PLGA based nanoparticles for sustained regional lymphatic drug delivery. *J Pharm Sci*. 2009;99:2018–2031.
27. Gref R, Minamitake Y, Peracchia MT, Trubetskoy V, Torchilin V, Langer R. Biodegradable long-circulating polymeric nanospheres. *Science*. 1994;263:1600–1603.
28. Bala I, Hariharan S, Kumar MN. PLGA nanoparticles in drug delivery: the state of the art. *Crit Rev Ther Drug Carrier Syst*. 2004;21:387–422.
29. Cun D, Jensen DK, Maltesen MJ, et al. High loading efficiency and sustained release of siRNA encapsulated in PLGA nanoparticles: quality by design optimization and characterization. *Eur J Pharm Biopharm*. 2010;77:26–35.
30. Gao K, Huang L. Nonviral methods for siRNA delivery. *Mol Pharm*. 2009;6:651–658.
31. Scheinman RI, Trivedi R, Vermillion S, Kompella UB. Functionalized STAT1 siRNA nanoparticles regress rheumatoid arthritis in a mouse model. *Nanomedicine (Lond)*. 2011;6: 1669–1682.
32. Amrite AC, Kompella UB. Size-dependent disposition of nanoparticles and microparticles following subconjunctival administration. *J Pharm Pharmacol*. 2005;57:1555–1563.
33. Gao W, Xiao Z, Radovic-Moreno A, Shi J, Langer R, Farokhzad OC. Progress in siRNA delivery using multifunctional nanoparticles. *Methods Mol Biol*. 2010;629:53–67.
34. Sundaram S, Roy SK, Ambati BK, Kompella UB. Surface-functionalized nanoparticles for targeted gene delivery across nasal respiratory epithelium. *FASEB J*. 2009;23:3752–3765.
35. Stechschulte SU, Joussen AM, von Recum HA, et al. Rapid ocular angiogenic control via naked DNA delivery to cornea. *Invest Ophthalmol Vis Sci*. 2001;42:1975–1979.
36. Shen J, Samul R, Silva RL, et al. Suppression of ocular neovascularization with siRNA targeting VEGF receptor 1. *Gene Ther*. 2006;13:225–234.
37. Xia XB, Xiong SQ, Song WT, Luo J, Wang YK, Zhou RR. Inhibition of retinal neovascularization by siRNA targeting VEGF(165). *Mol Vis*. 2008;14:1965–1973.

38. Rao DD, Vorhies JS, Senzer N, Nemunaitis J. siRNA vs. shRNA: similarities and differences. *Adv Drug Deliv Rev*. 2009;61:746–759.
39. Kleinman ME, Yamada K, Takeda A, et al. Sequence- and target-independent angiogenesis suppression by siRNA via TLR3. *Nature*. 2008;452:591–597.
40. Kim DH, Behlke MA, Rose SD, Chang MS, Choi S, Rossi JJ. Synthetic dsRNA Dicer substrates enhance RNAi potency and efficacy. *Nat Biotechnol*. 2005;23:222–226.
41. Marques JT, Devosse T, Wang D, et al. A structural basis for discriminating between self and nonself double-stranded RNAs in mammalian cells. *Nat Biotechnol*. 2006;24:559–565.
42. Mukerjee A, Shankardas J, Ranjan AP, Vishwanatha JK. Efficient nanoparticle mediated sustained RNA interference in human primary endothelial cells. *Nanotechnology*. 2011;22:445101.
43. Amrite AC, Edelhauser HF, Singh SR, Kompella UB. Effect of circulation on the disposition and ocular tissue distribution of 20 nm nanoparticles after periocular administration. *Mol Vis*. 2008;14:150–160.
44. Ge YL, Zhang X, Zhang JY, Hou L, Tian RH. The mechanisms on apoptosis by inhibiting VEGF expression in human breast cancer cells. *Int Immunopharmacol*. 2009;9:389–395.
45. Cun D, Jensen DK, Maltesen MJ, et al. High loading efficiency and sustained release of siRNA encapsulated in PLGA nanoparticles: quality by design optimization and characterization. *Eur J Pharm Biopharm*. 2011;77:26–35.
46. Sundaram S, Trivedi R, Durairaj C, Ramesh R, Ambati BK, Kompella UB. Targeted drug and gene delivery systems for lung cancer therapy. *Clin Cancer Res*. 2009;15:7299–7308.